14

From Simplicity to Complexity and Back*

Function, Architecture, and Mechanism of Light-harvesting Systems in Photosynthetic Bacteria

K. SCHULTEN

Beckman Institute and Department of Physics, University of Illinois at Urbana-Champaign, Urbana, IL 61801, U.S.A.

*"... quod verum simplex sincerumque sit, id esse naturae hominis aptissimum."
— Cicero (De Officiis, 1,13)
[... what is true, simple, and pure is most fitted to the nature of man.]

ABSTRACT

Photosynthetic organisms fuel their metabolism with light energy and have developed for this purpose an efficient apparatus for harvesting sunlight, key features of which were conceptually established long ago. Recently, the atomic structure of a main protein constituent of the apparatus, as it evolved in purple bacteria, has been solved through a combination of modeling, X-ray crystallography, and electron microscopy. This permitted the modeling of the entire light-harvesting system, a complex nanometric aggregate of transmembrane proteins. This chapter discusses how an ongoing analysis has wrested an explanation of the light-harvesting function from an atomic level structure, based on quantum physics. The investigations of the light-harvesting system of purple bacteria demonstrate very clearly the course typical for research in biological physics, starting from a simply stated, known function and proceeding through experimental and theoretical investigations carried out at more and more refined levels of molecular reality: First, the macromolecular components of the system underlying a function are identified and their role characterized, e.g., through spectroscopy. Second, the complex

structures of these components are established at atomic resolution and functionally relevant architectural elements are recognized. Finally, through refined observation and theoretical analyses of these elements, the physical mechanisms exploited by the organism to achieve the function are determined.

INTRODUCTION

Living organisms are characterized through a remarkable set of facilities, for example, heredity and evolution, maintenance of a state of order through metabolic energy consumption, or information processing through chemical and electric signaling. These and other facilities were discovered initially on the basis of macroscopic observation or physiological experiments, and often an impressive degree of understanding was achieved at this level. Advances in crystallography, X-ray scattering, NMR, and electron microscopy in combination with arduous biochemical and physicochemical investigations have pushed the boundary of knowledge on the cell's machinery involved in the above-mentioned facilities from the level of organisms and cells to molecules, and ultimately to atomic level structures. However, such structures, welcomed and often heralded as great breakthroughs, are in themselves extremely complex and do not result promptly in deeper understanding. The step from often clearly and succinctly characterized, i.e., simple, cell functions to intrinsically complex protein structures needs to be succeeded by an attempt to regain clear and succinct descriptions of the mechanisms underlying the particular functions, which has often proven to be a long and difficult process.

Other chapters in this volume describe this process for the protein myoglobin, the structure of which was solved long ago. In this chapter, I investigate the journey from simplicity to complexity and back for a cellular function only recently characterized through atomic level structures: light harvesting in photosynthesis.

It is important to realize that this journey might pass across several levels of resolution of a biological organism. The least resolved level might be concerned with the establishment of cellular function. On the next level, the macromolecular components of the underlying system might be identified and their role characterized, e.g., through spectroscopy; still on a further level, the complex structures of these components might be established at atomic resolution and functionally relevant architectural elements might be recognized. On the final level, refined observation and theoretical analyses of these elements might determine the physical mechanisms exploited by an organism to achieve the cellular function.

The cellular apparatus involved in light harvesting will allow us to discuss how explanations of the mechanisms underlying the well-established function are wrested from complex protein structures and a conceptual foundation of cell biology grounded on the laws of physics is achieved. Since the proteins of the light-harvesting system furnish, in the first place, simply a scaffold for chromophores, the structure–function relationship is relatively more easy to state than in proteins undergoing dynamic processes and conformational transitions. However, the light-harvesting system studied

involves a nanometric aggregate of proteins, the size of which establishes a new level of complexity that is characteristic of many recently discovered biomolecular structures. In this regard, this chapter complements the focus on smaller proteins presented elsewhere in this volume. The light-harvesting system is also a harbinger of progress in research on bioelectronic systems, founded necessarily on quantum mechanical concepts.

In this chapter I initially outline the light-harvesting function as it was characterized many decades ago. I then describe the characterization of the components of the light-harvesting system, the establishment of the structures of the components as well as the whole photosynthetic unit (PSU), and recognition of the functionally relevant architectural elements. Finally, I outline the quantum mechanical description of these elements and the present perception of the physical mechanisms exploited by purple bacteria. This chapter follows closely the presentation in Hu et al. (1998).

FUNCTION AND PHYSICAL PRINCIPLES OF LIGHT HARVESTING

Photosynthetic life forms reduce CO_2 to carbohydrates by utilizing the energy of sunlight. The prevalent color of green in the Earth's biosphere is testimony to the important role that chlorophylls play in this regard. Chlorophylls are assisted in their role by carotenoids, also widely known through their coloration of petals and fruits in plants. Emerson and Arnold (1932) demonstrated that it requires hundreds of chlorophylls to reduce one molecule of CO_2 under saturating flashlight intensity. To explain the cooperative action of these chlorophylls, these authors postulated that only very few chlorophylls in the primary reaction site, termed the photosynthetic reaction center (RC), take part directly in photochemical reactions; most chlorophylls serve as light-harvesting antennae, capturing the sunlight and funneling electronic excitation towards the RC. This notion gave rise to the definition of the PSU as an ensemble of an RC with associated light-harvesting complexes containing up to 250 chlorophylls. The PSU absorbs sunlight, fuels its energy in the form of electronic excitation into a system of chlorophylls, which acts as a funnel that conducts the excitation to the RC. The suggestion became widely accepted when Duysens carried out a critical experiment in which excitation transfer between different chlorophylls was observed (Duysens 1952).

The notion of 250 chlorophylls absorbing sunlight and funneling its energy in the form of electronic excitation through the chlorophyll ensemble to the RC caught the attention of the physicists R. Oppenheimer and T. Förster. Half a century ago they demonstrated independently, through application of quantum mechanical perturbation theory, that molecules like chlorophylls can transfer among each other electronic excitation by means of induced dipole–induced dipole interaction. Förster's respective formula for the rate of transfer from donor D to acceptor A is widely used in spectroscopy today in the form:

$$k_{D \to A} = \frac{1}{\tau_D} \left(\frac{R_0}{R} \right)^6 , \qquad (14.1)$$

where τ_D is the radiative lifetime of D^* and R_0 is the so-called Förster radius, the length scale over which excitation transfer is efficient. R_0 is defined through

$$R_0^6 = \frac{c \kappa^2 \phi_D}{n^4} \int d\nu \ \nu^{-4} S_{D^*}(\nu) S_A(\nu) . \qquad (14.2)$$

Here, c is a system-independent constant, κ is a parameter dependent on the relative orientation of A and D, ϕ_D is the fluorescence quantum yield of D^*, n is the environmental optical density, and the spectral line shape functions $\widetilde{S}_{D^*}(\nu), S_A(\nu)$ account for the transitions $D^* \to D, A \to A^*$; $\widetilde{S}_{D^*}(\nu)$ is normalized as $\int \widetilde{S}_{D^*}(\nu) d\nu = 1$, whereas $S_A(\nu)$ represents an extinction coefficient.

Equation 14.1 is based on a multipole expansion, accounting for dipolar contributions, and actually applies only when the distance between the edges of A and D is much larger than the overall size of the molecules themselves. For such geometry, the Förster formula predicts that excitation transfer arises only when the transitions $D^* \to D, A \to A^*$ are both optically allowed. When the stated geometrical criteria are not met, the latter is not a precondition for excitation transfer and even optically forbidden transitions can be participants in the process. For a general description one cannot, therefore, rely on a multipole expansion, but rather one needs to account in a numerical calculation for the complete Coulomb coupling between donor and acceptor electronic states. Below I refer to the respective situation as being governed by the Coulomb mechanism.

In 1953, Dexter pointed out that a second mechanism exists for excitation transfer, which is based on electron exchange between donor D and acceptor A (Dexter 1953) and which has been described in detail for light harvesting in purple bacteria by Damjanovic et al. (1999). The Coulomb and exchange mechanisms for excitation transfer differ significantly in their operative range. While the Coulomb mechanism is effective over distances of typically 20–50 Å, the exchange mechanism is effective only when there is sufficient overlap of the wave functions of D^* and A, i.e., for distances of a few Å. The Coulomb mechanism, for optically allowed transitions, has an R^{-6} distance dependence as described by Equation 14.1, with a typical operational range R_0 of 30 Å. The exchange mechanism decays exponentially with distance; for it to be effective, donor and acceptor must be in direct contact.

As a consequence of selection rules, the Coulomb mechanism applies only to the transfer of singlet excitations (assuming singlet ground states of A and D), whereas the exchange mechanism is applicable also to the transfer of triplet excitations (Damjanovic et al. 1999). Using the Dexter mechanism, the carotenoids can protect the bacteriochlorophylls (BChls) and the entire bacterium against the detrimental effects of BChl triplet states which arise with a small but finite probability and can generate excited oxygen according to the reaction $^3O_2 + {}^3BChl^* \to {}^1O_2^* + {}^1BChl$. The carotenoids quench the BChl triplet states and, as a result, electronic excitation of O_2 is

prevented and with it the damaging properties of this compound in its reactive singlet form.

The successful implication of the basic laws of physics in the suggested light-harvesting function by the mentioned researchers and others (e.g., Knox 1963) posed a clear challenge to another generation of scientists to discover the architecture of the PSU at a level of detail that would permit the application of quantum physics to deduce observed properties and understand its mechanism.

LIGHT HARVESTING IN PHOTOSYNTHESIS IN PURPLE BACTERIA

In the following, we jump to the discovery of the organization of the photosynthetic unit of one particular photosynthetic species: purple bacteria. Not mentioned are decades of research leading to the preparation of the system, to spectroscopic observations of excitation transfer down to the femtosecond time scale, and to a more complete theoretical understanding of molecular energy transfer. Figure 14.1 depicts schematically the intracytoplasmic membrane of purple bacteria with its primary photosynthetic apparatus. In the PSU, an array of light-harvesting complexes captures light and transfers the excitation energy to the photosynthetic RC. The latter is used to separate electron/hole pairs and to attract protons, reducing quinone, Q, to hydroquinone, QH_2. For this purpose, Q needs to shuttle into the RC and QH_2 out of the RC. The holes are replaced by electrons furnished by cytochrome c_2. The remaining part of the primary photosynthetic apparatus utilizes QH_2 to generate, by means of the bc_1 complex, a proton gradient which drives the synthesis of ATP.

The PSU of most purple bacteria contains two types of light-harvesting complexes: light-harvesting complex I (LH-I) and light-harvesting complex II (LH-II) (Zuber and Brunisholz 1991). LH-I is found directly surrounding the RCs (Miller 1982; Walz and Ghosh 1997), while LH-II is not in direct contact with the RC but transfers energy to the RC via LH-I (Monger and Parson 1977; van Grondelle et al. 1994). For some bacteria, such as *Rhodopseudomonas* (*Rps*.) *acidophila* and *Rhodospirillum* (*Rs*.) *molischianum* strain DSM 120 (Germeroth et al. 1993), there exists a third type of light-harvesting complex, LH-III. A 1:1 stoichiometry is found between RC and LH-I (Walz and Ghosh 1997); the number of LH-IIs and LH-IIIs varies according to growth conditions, such as light intensity and temperature (Aagaard and Sistrom 1972).

Figure 14.2 shows the energy levels for the key electronic excitations in the PSU of purple bacteria. The energy levels reveal two types of components of light harvesting: components involving carotenoids and BChls, which fuel photons into the PSU as electronic excitations of BChl, and components involving solely the BChls that funnel the latter excitations to the RC. The photon-fueling components absorb light mainly at wavelengths of about 500 nm through carotenoids and above 800 nm through BChls, transferring the resulting excitations to the BChls forming the excitation funnel. LH-I, LH-II, and LH-III contain carotenoids, but only LH-II and LH-III contain a set of
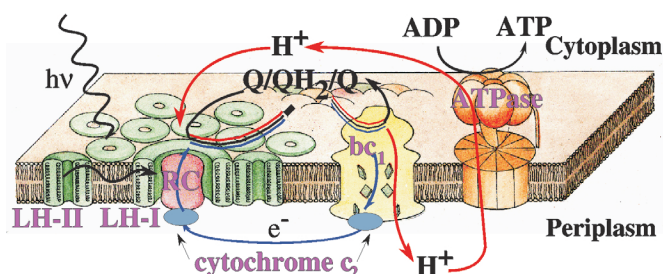
Figure 14.1 Schematic representation of the photosynthetic apparatus in the intracytoplasmic membrane of purple bacteria. The reaction center (RC, red) is surrounded by the light-harvesting complex I (LH-I, green) to form the LH-I–RC complex, which is surrounded by multiple light-harvesting complexes LH-II (green), forming altogether the photosynthetic unit (PSU). Photons are absorbed by the light-harvesting complexes and excitation is transferred to the RC initiating a charge (electron-hole) separation. The RC binds quinone Q_B, reduces it to hydroquinone Q_BH_2, and releases the latter. Q_BH_2 is oxidized by the bc_1 complex, which uses the exothermic reaction to pump protons across the membrane; electrons are shuttled back to the RC by the cytochrome c_2 complex (blue) from the ubiquinone-cytochrome bc_1 complex (yellow). The electron transfer across the membrane produces a large proton gradient that drives the synthesis of ATP from ADP by the ATPase (orange). Electron flow is represented in blue, proton flow in red, and quinone flow — likely confined to the intramembrane space — in black.

BChls absorbing at B800. The excitation funnel BChls are characterized through a pronounced energetic hierarchy: the respective BChls in LH-III at the periphery of the PSU absorb at 820 nm, the ones in the more central LH-II absorb at 850 nm, and the ones in LH-I in contact with the RC absorb at 875 nm (van Grondelle et al. 1994). This energy cascade, according to the principles of thermodynamcis, serves to funnel electronic excitations from the LH-IIIs and LH-IIs through LH-I to the RC. Time-resolved picosecond and femtosecond spectroscopy revealed that excitation transfer within the PSU occurs on a subpicosecond (in the photon-fueling components) to picosecond (in the excitation funnel components) time scale and altogether at near unit (95%) efficiency (Pullerits and Sundstrom 1996; Fleming and van Grondelle 1997).

   The photon fueling/excitation funnel system in Figure 14.2 constitutes a detailed, yet conceptually simple, picture of light harvesting in purple bacteria. The picture combines knowledge of the constituents of the system with measured transfer pathways and rates (not shown) in a physically sensible scheme. One could consider this picture a satisfactory explanation for light harvesting, but it still leaves unanswered the questions: How exactly are the chlorophylls and carotenoids organized in the PSU, and how does the system achieve its high efficiency? These questions become more serious if one compares light-harvesting systems of different photosynthetic life forms which show little resemblance. Is there a common ancestor to the PSUs of all photosynthetic life, and what factors might have caused evolutionary divergence? Such answers require a deeper knowledge of the molecular machinery behind Figure 14.1.
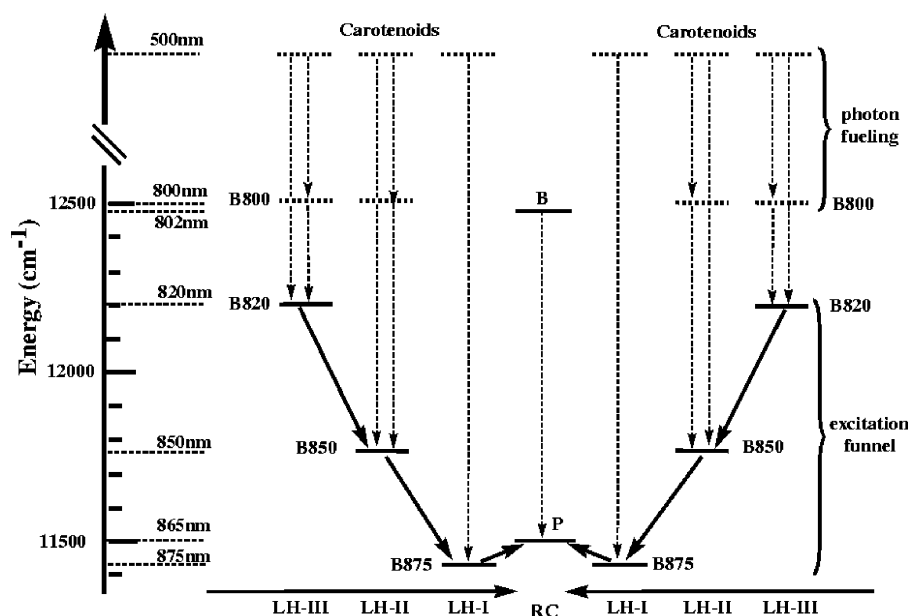
Figure 14.2 Energy levels of the electronic excitations in the PSU of BChl *a* containing purple bacteria. The diagram illustrates a funneling of excitation energy towards the photosynthetic reaction center (RC). The dashed lines indicate (vertical) intra-complex excitation transfer; the solid lines (diagonal) inter-complex excitation transfer. LH-I exists in all purple bacteria; LH-II exists in most species; LH-III arises in certain species only.

STRUCTURAL MODEL OF THE PSU OF
RHODOBACTER SPHAEROIDES

The PSU is a nanometric aggregate of many components and as such it poses an extreme challenge for structure analysis methods available today. Figure 14.3 presents a structural model of the PSU for the purple bacterium *Rhodobacter* (*Rb*.) *sphaeroides*. Shown is a top view of an RC, surrounded by a (large) ring-like protein, the light-harvesting complex I (LH-I) with a 16-fold symmetry axis, which in turn is surrounded by (small) ring-like proteins, the light-harvesting complex II (LH-II) with a ninefold symmetry axis. Only three LH-IIs are shown. The actual photosynthetic apparatus can contain up to about nine LH-IIs around each LH-I, a number derived from observed stoichiometries as well as concluded from the assumption that nine LH-IIs fit around LH-I, leaving a sufficient opening for Q/QH_2 shuttling.

All components in Figure 14.3, except the RC, have been modeled from homologous proteins as explained below. Even though only a model of the PSU is presented here, I wish to stress that for the purposes of the central mechanism of light harvesting, the model is likely satisfactory and as good as a real structure.
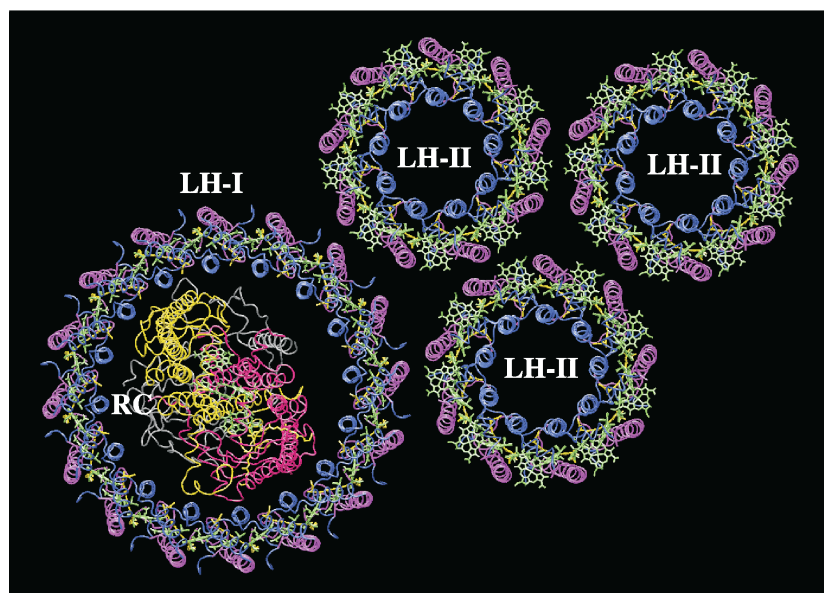
Figure 14.3 Arrangement of pigment protein complexes in the modeled bacterial photosynthetic unit (PSU) of *Rb. sphaeroides*. The α-helices are represented as C_α-tracing tubes with α-apoproteins of both LH-I and LH-II in blue and β-apoproteins in magenta, and the L, M, and H subunits of RC in yellow, red, and gray, respectively. All the BChls are in green, and carotenoids in yellow. (Produced with the program VMD [Humphrey et al. 1996]).

Molecular biologists critical of modeling are reminded that other disciplines employ models routinely and successfully (e.g., condensed matter physics) and have learned to judge the benefits as well as the shortcomings of models. Certainly, it is more desirable to base conclusions on a highly resolved structure of the PSU at below 1 Å resolution (the relevant length scale relevant for a faithful quantum mechanical description of light harvesting) and in the form of a movie with 100 fs time resolution (the physically relevant time scale); however, since this information is not available, and may never be due to the naturally disordered character of a cell membrane or a thermal protein, a computational model must suffice. Theoretical biology has invested much effort in extrapolating structure and dynamics from homologous and static structures by means of many types of model building algorithms as well as molecular dynamics; such tools, as well as bioinformatics methodologies, have been employed to derive the structure shown in Figure 14.3 (Hu and Schulten 1998; Hu et al. 1998).

In the PSU of *Rb. sphaeroides*, the structure of the photosynthetic RC is known (Ermler et al. 1994). In fact, the availability of this structure prompts us here to model the PSU of this species, rather than that of another species. Since we are presently concerned with the light-harvesting function, we will not discuss the structure of the RC further, except later in regard to its function as an acceptor of electronic excitation.

The structure of LH-II for *Rb. sphaeroides* is not known, but it has been determined for *Rps. acidophila* (McDermott et al. 1995) and for *Rs. molischianum* (Koepke et al. 1996). For the latter species the structure, determined to 2.4 Å resolution (Koepke et al. 1996), is shown in Figure 14.4a. The protein is an octameric aggregate of αβ-heterodimers; the latter contain a pair of short peptides (α- and β-apoproteins) noncovalently binding three BChl *a* molecules and one lycopene (a specific type of carotenoid). Presumably, a second lycopene exists for each αβ-heterodimer. The electron density map exhibits indeed a stretch of assignable density, but not long enough to resolve the entire lycopene (Koepke et al. 1996). Two concentric cylinders of α-helices, with the α-apoproteins inside and the β-apoproteins outside, form a scaffold for BChls and lycopenes. Figure 14.4b depicts the 24 BChl molecules and eight lycopene molecules in LH-II with all other components stripped away. Sixteen B850 BChl molecules form a continuous overlapping ring of 23 Å radius (based on central Mg atoms of BChls) with each BChl oriented perpendicular to the membrane plane. The Mg–Mg distance between neighboring B850a and B850b BChls is 9.2 Å (within an αβ-heterodimer, cf. Figure 14.4) and between B85Oa′ and B850b is 8.9 Å (between heterodimers, cf. Figure 14.4). Eight B800 BChls, forming another ring of 28 Å radius, are arranged with their tetrapyrrol rings nearly parallel to the membrane plane and exhibit a Mg–Mg distance of 22 Å between neighboring BChls, i.e., the BChls are coupled only weakly. The ligation sites for the B850 BChl are α-His-34 and β-His-35, while the B800 BChls ligate to α-Asp-6. Eight lycopene molecules are found to span the transmembrane region, each making close contact with a B800 BChl and a B850a BChl.

The structure of LH-II of *Rb. sphaeroides* has not yet been determined through crystallography. The α- and β-apoproteins of this protein exhibit a close homology to the subunits of LH-II from *Rps. acidophila*: α-apoprotein has 45% sequence identity with its *Rb. sphaeroides* counterpart, the transmembrane segment of the β-apoprotein has 65% sequence identity. Electron microscopy observations suggest that LH-II of *Rb. sphaeroides* contains nine αβ-heterodimers (Olsen, pers. comm.), instead of eight as in LH-II of *Rs. molischianum*. LH-II of *Rb. sphaeroides*, as shown in Figure 14.3, has been constructed, therefore, as a nanomer of αβ-heterodimers by means of homology modeling using the αβ-heterodimer of LH-II from *Rps. acidophila* as a template. For this purpose, the modeling protocol developed and applied successfully to LH-II of *Rs. molischianum* in Koepke et al. (1996), Hu et al. (1995a), and Hu and Schulten (1998) was utilized.

The structure of LH-I of *Rb. sphaeroides* and of its complex with RC are also not yet available. However, electron micrographs of the protein alone as well as in complex with RC (R. Ghosh, pers. comm.) exist. The protein exhibits a ring-like structure with a 16-fold symmetry axis, the degree of symmetry being apparently subject to sample preparation and possibly to data-averaging procedures. In particular, the complex with RC can show a deformation from a 16-fold symmetry, e.g., a 4-fold symmetry (R. Ghosh, pers. comm.). Actually, Jungas et al. (1999) provide electron micrographs for *Rb. sphaeroides* that reveal an aggregate of two half-circular LH-Is with two RCs. For
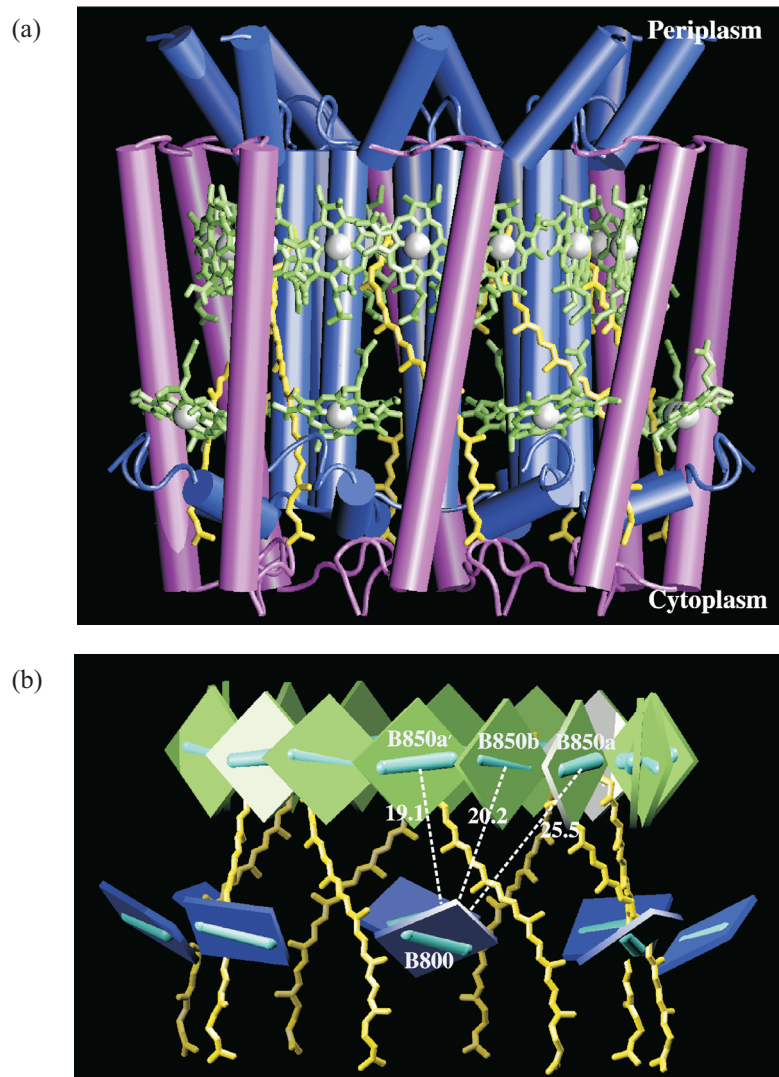
Figure 14.4 The octameric LH-II complex from *Rs. molischianum* (from Koepke et al. 1996). (a) The α-helical segments are represented as cylinders with the α-apoproteins (inside) in blue and the β-apoprotein (outside) in magenta. The BChl molecules are in green with phytyl tails truncated for clarity. The lycopenes are in yellow. (b) Arrangement of chromophores with BChls represented as squares, and with carotenoids (lycopenes) in a licorice representation. Bars connected with the BChls represent the Q_y transition dipole moments as defined by the vector connecting the N atom of pyrrol I and the N atom of pyrrol III (Gouterman 1961). Representative distances between central Mg atoms of B800 BChl and B850 BChl are given in Å. The B850 BChls bound to the α-apoprotein and the β-apoprotein are denoted as B850a and B850b, respectively; BChl B850a′ is bound to the (left) neighboring heterodimer.

the purpose of developing a description of the PSU of *Rb. sphaeroides*, we adopt the model of LH-I as derived in Hu and Schulten (1998), which involves a hexadecamer of αβ-heterodimers; the modeling exploited a close homology of these heterodimers to those of LH-II of *Rs. molischianum*. The resulting LH-I structure yields an electron density projection map that is in agreement with an 8.5 Å resolution electron microscopy projection map for the highly homologous LH-I of *Rhodospirillum rubrum* (Karrasch et al. 1995). The LH-I complex contains a ring of 32 BChls referred to as B875 BChls according to their main absorption band. The Mg–Mg distance between neighboring B875 BChls is 9.2 Å within the αβ-heterodimer and 9.3 Å between neighboring heterodimers.

The modeled LH-I has been docked to the photosynthetic RC of *Rb. sphaeroides* by means of a constrained conformational search (Hu and Schulten 1998), employing for the RC the structure reported in Ermler et al. (1994). Figure 14.5a, b presents the LH-I–RC complex. The arrangement of the BChls in the LH-I–RC complex is depicted in Figure 14.4b. One can discern the ring of B875 BChls of LH-I that surrounds the reaction center special pair (P_A and P_B) and the so-called accessory BChls (B_A, B_B). The closest distance between the central Mg atom of the RC's special pair (bacteriochlorophylls P_A and P_B) and the Mg atom of the BChls in LH-I is 42 Å. The distance between the Mg atom of the accessory BChl (bacteriochlorophylls B_A, B_B) and the LH-I BChls is shorter, the nearest distance measuring 35 Å. *Rb. sphaeroides* contains an additional *Puf*X gene. It has been suggested that the *Puf*X protein substitutes one or more αβ-heterodimers of LH-I to open up the circular ring shown in Figure 14.4a and to facilitate, thereby, the flow of quinones (Q_B/Q_BH_2) between the RC and the cytochrome bc_1 complex (see Figure 14.1) (Farchaus and Oesterhelt 1989; Cogdell et al. 1996; Walz and Ghosh 1997). A preliminary model of a *Puf*X dimer, replacing a single LH-I heterodimer, exhibits an opening suitable for the RC-bound quinone (cf. Figure 14.5a) to shuttle out of the LH-I–RC complex.

ARRANGEMENT OF CHROMOPHORES IN THE PSU

The PSU is a protein aggregate of overwhelming complexity. The task of connecting its structure to the photon fueling/excitation funnel function, as depicted in Figure 14.2, appears formidable. However, the light-harvesting proteins in the PSU serve mainly a structural role, as a scaffold for the chlorophyll and carotenoid chromophores. Discarding the peptide components of the PSU results in the arrangement of chromophores as shown in Figure 14.6. One can discern a hierarchical aggregate of the BChls, organized into rings of 18 closely coupled (B850) and nine loosely coupled (B800) BChls in the peripheral LH-IIs surrounding a large ring of 32 closely coupled (B875) BChls of LH-I which in turn surrounds four chlorophylls of RC. Close groupings, shown separately in Figure 14.7, of carotenoids with three LH-II BChls can also be recognized.

(a)

(b)
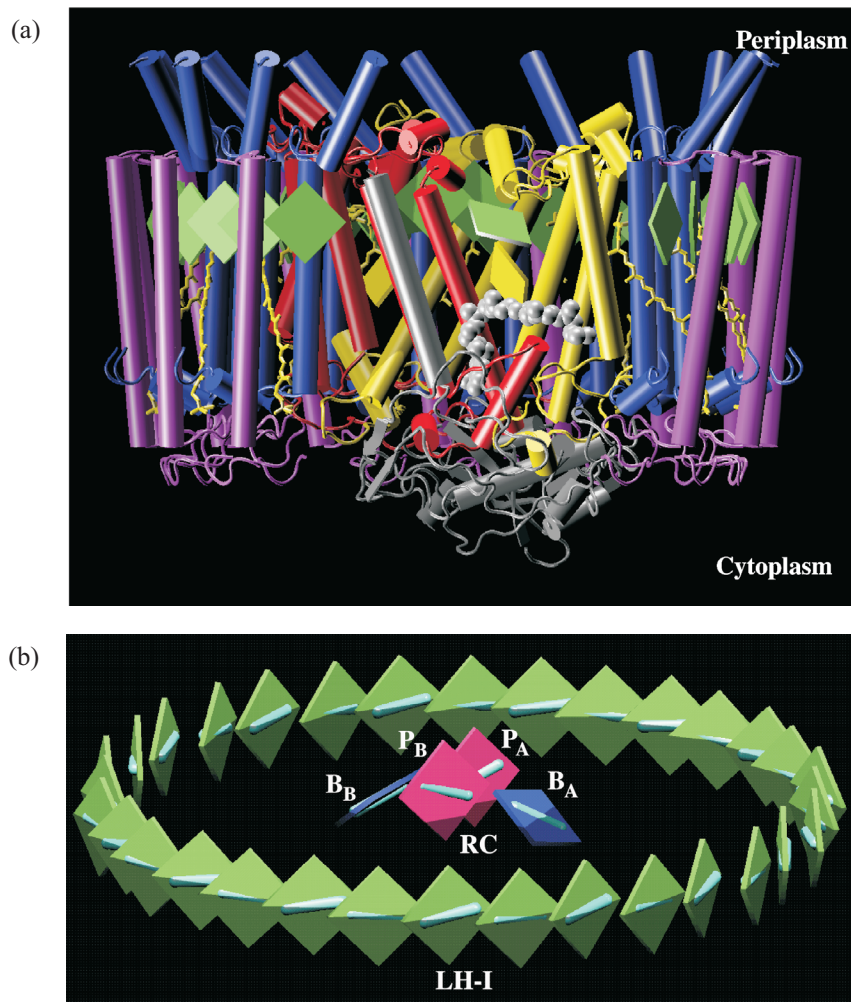
Figure 14.5 Structure of the LH-I–RC complex. (a) Side view of the LH-I–RC complex with three LH-I $\alpha\beta$-heterodimers on the front side removed to expose the RC in the interior. The α-helices are represented as cylinders with the L, M, and H subunits of the RC in yellow, red, and gray, and the α-apoprotein and the β-apoprotein of the LH-I in blue and magenta. BChls and bacteriopheophytins are represented as green and yellow squares, respectively. Carotenoids (spheroidenes) are in a yellow licorice representation, and quinone, Q_B, is rendered by gray van der Waals spheres. Q_B shuttles in and out (as Q_BH_2) of the LH-I–RC complex, as indicated in Figure 14.1. (b) Arrangement of BChls in the LH-I–RC complex. The BChls are represented as squares with B875 BChls of LH-I in green, and the special pair (P_A and P_B) and the accessory BChls (B_A and B_B) of the RC in red and blue, respectively; cyan bars represent Q_y transition moments of BChls. (Produced with the program VMD [Humphrey et al. 1996]).
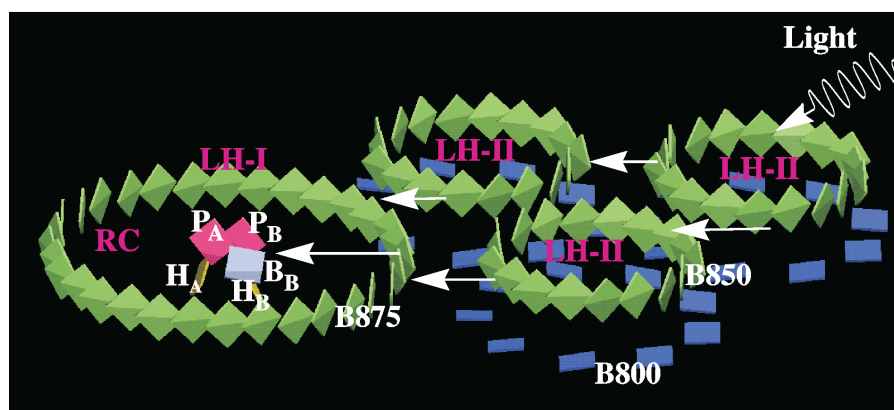
Figure 14.6 Excitation transfer in the bacterial photosynthetic unit. LH-II contains two types of BChls, commonly referred to as B800 (dark blue) and B850 (green), which absorb at 800 nm and 850 nm, respectively. BChls in LH-I absorb at 875 nm and are labeled B875 (green). P_A and P_B refer to the reaction center special pair, and B_A, B_B to the accessory BChls in the RC. The figure demonstrates the coplanar arrangement of the B850 BChl ring in LH-II, the B875 BChl ring of LH-I, and the reaction center BChls P_A, P_B, B_A, B_B. (Produced with the program VMD [Humphrey et al. 1996]).

An essential feature of the chromophore organization of the PSU is that the ring-like aggregates of BChls within LH-I and LH-II exhibit a coplanar arrangement together with the BChls in the RC. An analysis of the LH-I and LH-II structures (Hu and Schulten 1998; Hu et al. 1997) indicates that each BChl of the B850 ring of LH-II and of the B875 ring of LH-I is noncovalently bound to three side-chain atoms of the α- or β-apoprotein such that the BChls are held in a rigid orientation, underscoring the relevance of the arrangement shown in Figure 14.6.

The chromophore aggregate shown in Figure 14.6 is a structure of simplicity and beauty. One may want to conclude at this point that the structural model implies an obvious answer to the question posed by Figure 14.2, i.e., how photons are fueled into the BChl system and electronic excitation is funneled to the RC. It has long been observed that excitation transfer LH-II → LH-I → RC occurs in the PSU in less than 100 picoseconds and with about 95% efficiency (Pullerits and Sundstrom 1996). In this respect, it is interesting to note that the transition dipole moments of the Q_y excitations of the B850 and B875 BChls are all oriented in the two-dimensional plane that encompasses the ring-like BChl aggregates of LH-II, LH-I, and the RC special pair and is optimally attuned to the desired flow of electronic excitation LH-II → LH-I → RC. However, the intuitive appeal of the aggregate architecture in Figure 14.6 cannot be confused with a sound understanding, which requires that one applies the laws of physics to the chromophore aggregate shown and investigates the emergent properties as well as their relationship to the function of the PSU. The efficient transfer of electronic excitation from the periphery to the center is hardly a foregone conclusion, prompting the consideration of several issues.
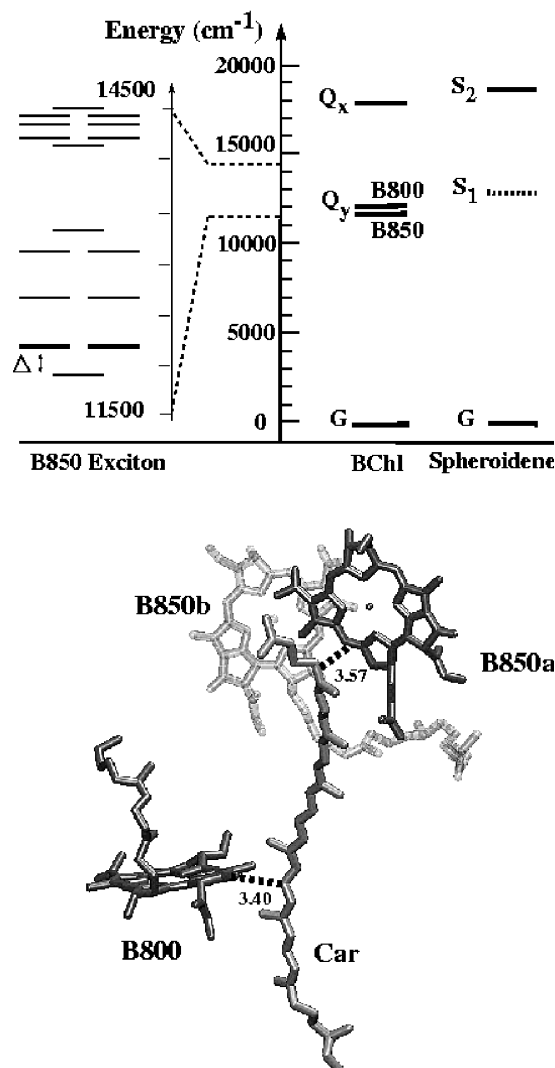
Figure 14.7 Bacteriochlorophyll–carotenoid interactions. Top left: Exciton bands of the circular B850 BChl aggregate as determined by quantum chemical (INDO/S) calculations (Zerner et al. 1998) based on coordinates of the crystal structure of LH-II from *Rs. molischianum* (Koepke et al. 1996). The degenerate states that carry all the oscillator strength are highlighted by thickened lines. Top right: excitation energies of BChl and carotenoid states in LH-II of *Rb. sphaeroides*. Solid lines represent spectroscopically measured energy levels. Dashed lines indicate the estimated (see Damjanovic et al. 1998; Nagae et al. 1993) energy for the optically forbidden S_1 state of the carotenoid spheroidene. Bottom: arrangement of spheroidene and the most proximate BChls based on the modeled structure of LH-II from *Rb. sphaeroides*. Close contacts between BChl and carotenoid spheroidene are indicated by representative distances (in Å).

First, one must concede that the system of 200–300 BChls and about 100 carotenoids is too large to be described *ab initio* on the basis of quantum physics. The system needs to be broken up into constituents, with proper justification that the necessary dissection does not essentially alter relevant properties. Fortunately, the aggregate shown exhibits a distinct hierarchy of spatial scales. BChls in the individual rings of LH-IIs, LH-I, and the RC are spatially closer and likely more tightly coupled than are BChls belonging to different units (rings, RC). One also notices that the so-called B800 BChls are themselves all spatially separated (center-to-center) by 20 Å and are likely well described as individual BChls. The carotenoids experience close contacts with certain BChls (see Figure 14.7) and the effect of the resulting interactions requires a detailed description. The dissection of the chromophore aggregate in the PSU conforms actually with quantum mechanical perturbation theory, which suggests how a hierarchy of interacting units can be composed from descriptions of its components. Perturbation theory is well tested and provides, in particular, criteria that determine its applicability.

Second, even the mentioned subcomponents are too large for a truly fundamental description. Rather, so-called semiempirical descriptions need to be invoked or so-called *ab initio* methods with a high degree of simplification, the choice of which implies also a strong empirical component. However, a satisfactory description should be one that has been previously and independently, i.e., in a separate context, applied successfully to homologous molecular systems. Since chlorophylls and carotenoids have been investigated intensely for decades by means of semiempirical methods, one treads here on fairly safe ground.

Third, one must note that the structure shown in Figure 14.6 is a static, stroboscopic view, and a highly idealized one in regard to the symmetry of the individual units. The actual system is subject to thermal motion which distorts the imposed symmetries. The LH-I ring surrounding the RC may actually be severely distorted in its shape by the RC or may be only a half-circle, as observed by Jungas et al. (1999). Furthermore, in some purple bacteria, one (or possibly more) of the sixteen units of LH-I is replaced by *Puf*X, which interrupts the ring of BChls to provide a gate through which Q_B/Q_BH_2 can be shuttled. The physical description achieved must be subjected to the mentioned distortions in order to discern which features of the description are robust against thermal motion and shape changes. The computational task involved in the suggested theoretical investigations is formidable, and the results necessarily complex. A simple finding is by no means certain.

QUANTUM MECHANICAL DESCRIPTION OF EXCITATION FUNNEL

One of the most intriguing structural features of the bacterial light-harvesting complexes is the circular organization of BChl aggregates (Hu and Schulten 1997). To understand the primary processes of light absorption and the subsequent excitation

transfer from LH-IIs, through LH-I, to the RC, it is essential to characterize the electronic properties of the excited states of a circular BChl aggregate. For this purpose we have carried out INDO-CIS (Zerner et al. 1998) calculations of individual BChl, small groupings of BChls as they occur in LH-II of *Rs. molischianum*, and of an entire circular aggregate of sixteen B850 BChls. The INDO-CIS method proved earlier to be satisfactory for the description of electronic excitations of organic chromophores, in particular, chlorophylls (Thompson and Zerner 1991). The low energy part of the spectrum resulting for the ring of sixteen B850 BChls is presented in Figure 14.7. The energy levels shown are mainly due to linear combinations of BChl Q_y excitations, so-called excitons. The two bands of the spectrum arise from a dimerization of the BChls in LH-II, i.e., B850a′ and B850b BChls are closer than B850a and B850b BChls as mentioned above (cf. Figure 14.4b).

A complete analysis of the INDO-CIS results also reveals higher energy excitations corresponding to Q_x states of individual BChls as well as to so-called charge resonance states. However, these states should not play a role for the excitation funnel since they are out of resonance with other relevant electronic excitations. Nonetheless, these states may absorb light and fuel its energy into the funnel system.

The B850 BChl spectrum in Figure 14.7 arises mainly from interactions between the BChl Q_y excitations of individual BChls. One may ask how far a reduced description (in terms of just these excitations) would reproduce the INDO-CIS results in which thousands of other excitations have been identified. Such a reduced description would be formulated in terms of a 16×16 Hamiltonian matrix $\langle j|\hat{H}|k \rangle$, where $|j\rangle$, $j = 1,...16$ represents the Q_y excitations of individual BChls. The diagonal elements $\langle j|\hat{H}|j \rangle = \varepsilon$ account for the excitation energy of the Q_y state. For non-nearest neighbor BChls j and k, associated interactions $\langle j|\hat{H}|k \rangle$ should be well approximated by dipole–dipole coupling terms:

$$\langle j|\hat{H}|k \rangle = C\left(\frac{\vec{d}_j \cdot \vec{d}_k}{r_{jk}^{\,3}} - \frac{3(\vec{r}_{jk} \cdot \vec{d}_j)(\vec{r}_{jk} \cdot \vec{d}_k)}{r_{jk}^{\,5}} \right), \, k \neq j, \, j \pm 1, \qquad (14.3)$$

where $\vec{d}_j$ are unit vectors describing the direction of the transition dipole moments of the ground state $\rightarrow Q_y$ state transition of the jth BChl and $\vec{r}_{jk}$ is the vector connecting the centers of BChl j and BChl k. C is a parameter, yet unspecified, related to the oscillator strength of the *ground state* $\rightarrow Q_y$ transition. The induced dipole–induced dipole coupling does not account well for interactions between neighboring BChls since the geometry criterion for the multipolar expansion is not met. Due to the eightfold symmetry of LH-II, the respective matrix elements $\langle j|\hat{H}|j+1 \rangle$ assume only two different values, namely, v_1 (v_2) for odd (even) j. The Hamiltonian is then specified through four parameters: ε, v_1, v_2, and C. These parameters can be chosen such that the spectrum resulting for the matrix $\langle j|\hat{H}|k \rangle$ reproduces closely the spectrum of a full INDO-CIS calculation. The corresponding parameters are $\varepsilon = 13{,}242$ cm^{-1}, $v_1 = 790$ cm^{-1}, $v_2 = 369$ cm^{-1}, and $C = 505{,}644$ Å^3 cm^{-1}.

The effective Hamiltonian reproduces the INDO-CI spectrum of the B850 BChls in LH-II well, except for the energy gap Δ (see Figure 14.6) between the lowest and second lowest excited state, which measures 422 cm^{-1}, i.e., twice the value predicted in a pure effective Hamiltonian picture. The reason for the difference is that the lowest electronic excitation experiences level repulsion with higher charge resonance states not accounted for by the effective Hamiltonian. Other calculations, less extensive than the INDO-CIS procedure in Zerner et al. (1998), ranging from alternative effective Hamiltonian representations (Dracheva et al. 1996; Hu et al. 1995b; Sauer et al. 1996) to the quantum mechanical consistent-force-field/π-electron (QCFF/PI) approach (Alden et al. 1997), yield a similar exciton band structure as INDO-CIS but differ in detailed exciton levels and band gaps.

A key feature of the electronic excitations connected with the B850 BChl spectrum in Figure 14.7 is the distribution of oscillator strength of the exciton states, i.e., the ability of the states to absorb or emit light directly. Only the energetically degenerate pair of states $|\tilde{2}\rangle, |\tilde{3}\rangle$ above the lowest energy state $|\tilde{1}\rangle$ carry nonzero oscillator strength. Due to a well-known sum rule, the addition of all oscillator strengths of the exciton band system, in the effective Hamiltonian description, must be equal to the sum of Q_y state oscillator strength D_y of the individual BChls (equal $16D_y$), i.e., $|\tilde{2}\rangle$ and $|\tilde{3}\rangle$ must each carry oscillator strength $8D_y$. This value reflects the property of the exciton states $|\tilde{2}\rangle, |\tilde{3}\rangle$ to be coherent superpositions of Q_y excitations $|j\rangle, j = 1,...16$ of individual BChls, just as the vanishing of oscillator strength of state $|\tilde{1}\rangle$ reflects a coherent spread of excitations around the entire BChl ring.

The distribution of oscillator strength can have important functional implications: excitation of the B850 BChl system would result, after thermal relaxation, in the preferential population of the energetically lowest exciton state $|\tilde{1}\rangle$, which is optically forbidden due to its vanishing oscillator strength and, hence, is prevented from wasteful fluorescence. The population of state $|\tilde{1}\rangle$ would depend sensitively on the actual energy difference Δ between $|\tilde{1}\rangle$ and the energetically degenerate states $|\tilde{2}\rangle, |\tilde{3}\rangle$.

One must note that the properties of the B850 BChl system outlined depend on the ideal eightfold symmetry axis of LH-II of *Rs. molischianum*. Distortions due to thermal motion or interruptions of the complete circle would alter the oscillator strength distribution. The characteristics of the exciton states due to a complete coherent spread of the excitations over the LH-II ring need to be studied in the presence of distortions. It is widely believed that the B850 BChl excited states, despite natural disorder, are delocalized; however, the extent of delocalization is debated (Fleming and van Grondelle 1997). The estimate for the number of coherently coupled BChls ranges from two BChl molecules (Jimenez et al. 1996) to the entire length of the B850 BChl aggregate (Wu et al. 1997; van Oijen et al. 1999). In principle, the relative strengths of the disorder and of the coupling between BChls determine the delocalization length. According to the effective Hamiltonian picture, the coupling between nearest neighbor BChls is 790 cm^{-1} (v_1) within the $\alpha\beta$-heterodimer, and 369 cm^{-1} (v_2) between the

αβ-heterodimers (see above). The effect of static disorder has been modeled in Hu et al. (1997) by randomizing the diagonal elements of an effective Hamiltonian and carrying out an effective Hamiltonian description numerically for a large ensemble of randomized Hamiltonians. Using a distribution consistent with the inhomogeneous broadening measured by hole-burning spectroscopy, the effect of diagonal disorder on exciton delocalization and oscillator strength distribution was found to be noticeable, but small. Static off-diagonal disorder shows similar effects (Schulten et al., unpublished results).

The treatment of dynamic disorder for an exciton system, like that of the Q_y excitons in LH-II, is technically extremely difficult and essentially impossible. One needs to describe respective systems mathematically in the product space of quantum states, Ω, and of stochastic states, Σ, i.e., in the very high-dimensional space $\Omega \otimes \Sigma$. Descriptions achieved so far restrict Σ to two states (Barvík et al. 1998). Desirable would be a sampling of an effective state space of the B850 BChl ring in LH-II through a molecular dynamics simulation, abstraction of a stochastic operator which would account for the monitored transitions between stochastic states, and a subsequent stochastic quantum mechanical description. For two-state quantum systems, such treatment has been achieved in Bittl and Schulten (1988, 1989), Schulten and Tesch (1991), and Xu and Schulten (1994).

The state of the quantum mechanical description of the B850 BChl ring in LH-II is still marred by the type of complexity that often arises in a still incomplete investigation. More refined *ab initio* quantum chemical calculations — including the effect of electron exchange between BChls, which is not accounted for in an INDO-CIS treatment nor in studies of static and dynamic randomization, all in close comparison with optical spectroscopy data — need to shed light on the issue of how localized or delocalized excitons in the B850 BChl ring actually are. Below, for the sake of argument, we assume that the description achieved in Zerner et al. (1998) and Hu et al. (1997) and the associated effective Hamiltonian description outlined are satisfactory.

EFFECTIVE HAMILTONIAN FOR EXCITATION FUNNEL

The effective Hamiltonian introduced above for LH-II of *Rs. molischianum* can be readily extended to describe the ring of 18 BChls in LH-II of *Rb. sphaeroides* as well as the ring of 32 BChls in LH-I of this species (Hu et al. 1997; Ritz et al. 1998). If one assumes that the nearest neighbor coupling in these light-harvesting complexes is the same as in LH-II of *Rs. molischianum*, i.e., v_1 and v_2, one can generalize the effective Hamiltonian without any further parameters, only the dimension of the matrix and the coordinates of the respective ring geometries, which enter Equation 14.3, need to be adjusted. The general form of the effective Hamiltonian is:

$$\hat{H} = \begin{pmatrix} \varepsilon & \nu_1 & W_{1,3} & W_{1,4} & \cdot & \cdot & \cdot & & \cdot & & W_{1,2N-1} & & \nu_2 \\ \nu_1 & \varepsilon & \nu_2 & W_{2,4} & \cdot & \cdot & \cdot & & \cdot & & W_{2,2N-1} & & W_{2,2N} \\ W_{3,1} & \nu_2 & \varepsilon & \nu_1 & \cdot & \cdot & \cdot & & \cdot & & W_{3,2N-1} & & W_{3,2N} \\ W_{4,1} & W_{4,2} & \nu_1 & \varepsilon & \cdot & \cdot & \cdot & & \cdot & & \cdot & & \cdot \\ \cdot & \cdot & \cdot & \cdot & \cdot & \cdot & \cdot & & \cdot & & \cdot & & \cdot \\ \cdot & \cdot & \cdot & \cdot & \cdot & \cdot & \cdot & & \cdot & & \cdot & & \cdot \\ \cdot & \cdot & \cdot & \cdot & \cdot & \cdot & \cdot & & \cdot & & \cdot & & \cdot \\ \cdot & \cdot & \cdot & \cdot & \cdot & \cdot & \cdot & & \varepsilon & & \nu_2 & & W_{2,2N-2,2N} \\ \cdot & \cdot & \cdot & \cdot & \cdot & \cdot & \cdot & & \nu_2 & & \varepsilon & & \nu_1 \\ \nu_2 & \cdot & \cdot & \cdot & \cdot & \cdot & \cdot & W_{2N,2N-2} & & & \nu_1 & & \varepsilon \end{pmatrix} \qquad (14.4)$$

Here, ε represents the excitation energy of the Q_y state. The quantities $W_{j,k}$ correspond to the elements $\langle j|H|k \rangle$ and are given by Equation 14.3. In case of LH-II of *Rb. sphaeroides*, one chooses $N = 9$ and in case of LH-I, $N = 16$. In both cases this description yields the same characteristics of the exciton bands as for the B850 BChl aggregate of LH-II of *Rs. molischianum*: the second and the third exciton states carry all the oscillator strength, the lowest energy exciton state being optically forbidden (Hu et al. 1997).

One can even extend the effective Hamiltonian to describe the BChls of the entire PSU, including the BChls in RC. The form of the Hamiltonian is:

$$\hat{H} = \begin{pmatrix} \hat{R}_{11} & \hat{R}_{12} & \cdots & \hat{R}_{1M} \\ \hat{R}_{21} & \hat{R}_{22} & \cdots & \hat{R}_{2M} \\ \vdots & \vdots & \ddots & \vdots \\ \hat{R}_{M1} & \hat{R}_{M2} & \cdots & \hat{R}_{MM} \end{pmatrix} \qquad (14.5)$$

Here, the elements $\hat{R}_{jk}$ are themselves matrices. $\hat{R}_{jj}$ describes the subcomponents of the excitation funnel, i.e., several 18×18 matrices accounting for the B850 BChl rings, a 32×32 matrix describing the B875 BChl ring, and a 4×4 matrix describing the BChls in RC. The elements of the latter matrix would need to be properly adjusted, since the nearest neighbor couplings in RC differ from those in LH-I and LH-II. All non-nearest neighbor couplings as well as the elements of the matrices $\hat{R}_{jk}, j \neq k$, describing couplings between the BChl rings or between the B875 BChl ring and the RC BChls, are furnished through Equation 14.3.

The effective Hamiltonian (Equation 14.5) furnishes a simple description of the relevant electronic properties of the light-harvesting system that hides the complexity of the underlying system of hundreds of partaking electrons. The Hamiltonian has been employed in Hu et al. (1997) and Ritz et al. (1998) to determine the rates of transfer of electronic excitation between LH-IIs, between LH-II and LH-I, and between LH-I and RC, i.e., to describe the excitation funnel component of the PSU shown in Figure 14.7. The calculated time constants of 3.3 and 65 ps for the excitation transfer processes

LH-II $\rightarrow$ LH-I and LH-I $\rightarrow$ RC in *Rb. sphaeroides*, respectively, are in agreement with experimental values of 3 ~ 5 ps and 35 ps (Hess et al. 1995; Visscher et al. 1989). A startling result from these calculations has been a suggested role of the accessory BChls as mediators of the excitation transfer from LH-I to the RC special pair: the calculated time for LH-I $\rightarrow$ RC transfer, in the absence of accessory BChls, is about 600 ps, which is an order of magnitude too long compared with observations; the accessory BChls in RC provide a tunneling path for the excitation transfer which bridges the large distance of 42 Å or longer between LH-I BChls and the RC special pair.

ROLE OF B800 BCHLS AND CAROTENOIDS
IN PHOTON FUELING

The energy of photons is fueled into the light-harvesting system through primary absorption by the B800 BChls and by the carotenoids. First, I will discuss the role of the B800 BChls and then that of the carotenoids.

The B800 BChls are oriented such that they absorb light in a direction perpendicular to that of the B850 BChls. The individual B800 BChls can transfer the resulting excitation energy to the B850 ring through the Förster mechanism (Oppenheimer 1941; Förster 1948). The transfer proceeds within 700 fs (Shreve et al. 1991). Quantum chemical calculations in Zerner et al. (1998) have demonstrated that the B800 BChls are only weakly coupled with each other and with the B850 BChls, a property also revealed by single-molecule spectroscopy (van Oijen et al. 1999). Calculations of excitation transfer in Damjanovic et al. (1999) reveal that the short transfer time, to a large degree, results from the exciton splitting of the accepting B850 exciton levels shown in Figure 14.6; the exciton splitting greatly improves the resonance of the excitations of B800 and B850 BChls.

Carotenoids absorb light at 500 nm into a strongly allowed state and transfer the excitation energy within 200 fs and with nearly 100% efficiency to the Q_y exciton states of the B850 ring (Chadwick et al. 1987). The question arises by which pathways and by which mechanism such an efficient excitation transfer is achieved. Figure 14.7 presents the energies of the excited states of spheroidene, the carotenoid in LH-II of *Rb. sphaeroides*, and of the BChls in LH-II of *Rb. sphaeroides*. Spheroidene features a strongly allowed singlet-excited state absorbing at 500 nm, labeled S_2, and a lower lying optically forbidden state labeled S_1. The latter state plays a prominent role and has been characterized by Hudson et al. (1982) and Tavan and Schulten (1987). In fact, the state S_2, which initially absorbs the 500 nm photons, decays within less than 200 fs into S_1. The S_1 state is in resonance with the accepting Q_y exciton states and, thus, provides a gateway for transfer to the B850 ring.

The optically forbidden character of the S_1 state of spheroidene precludes its coupling to the B850 ring through the Förster mechanism, thus limiting potential mechanisms to coupling through Coulomb interaction including higher-order multipoles or coupling through electron exchange (Dexter mechanism; Dexter 1953). Both transfer

routes require a close proximity between spheroidenes and BChls. Spheroidene and BChls are indeed found in close contact, as shown in Figure 14.7. Calculations based on the geometric arrangement of carotenoids and BChls in LH-II (Figure 14.7) and on CI expansions of the electronic states of carotenoids and chlorophylls, reported in Nagae et al. (1993) and Damjanovic et al. (1998), however, suggest that the exchange mechanism is largely ineffective since the respective coupling strength is very small. These calculations showed that the Coulomb mechanism results in a transfer of singlet excitations through the S_1 (carotenoid) $\rightarrow$ B850 (exciton states) pathway. This transfer is also strongly accelerated by the splitting of the B850 exciton levels (Damjanovic et al. 1999).

In addition to transfer through the forbidden S_1 state of spheroidene, the absorbing S_2 state of carotenoids transfers excitation directly to the Q_x state of BChl as suggested by the calculations in Damjanovic et al. (1999) and the shortened (60 fs) *in vivo* lifetime of the S_2 state in LH-II (Ricci et al. 1996).

Besides the light-harvesting function, carotenoids protect the light-harvesting system from the damaging effect of BChl triplet states as pointed out above. Carotenoids quench the BChl triplet states through triplet excitation transfer from the BChls. This transfer involves a spin change and can only proceed through the electron exchange mechanism (Dexter 1953). The triplet excitation transfer in LH-II of *Rs. molischianum* has been described in detail (Damjanovic et al. 1999). The calculations showed that B850a is well protected by one of the eight lycopenes seen in the crystal structure of LH-II of *Rs. molischianum* (see Figures 14.4 and 14.7), while B850b is not directly protected, but can transfer triplet excitation within a few picoseconds to the well-protected B850a BChl. The motif that BChls are protected via a bridge involving a further BChl has been found also in the RC (Laible et al. 1998) and in the light-harvesting complex of plants LHC-II (Kuhlbrandt 1994). B800 may need not be protected since it transfers its singlet excitation within ~1 ps to the B850 BChls.

HOW IS THE PSU ASSEMBLED *IN SITU*?

The remarkable overall architecture of the PSU is matched by the equally remarkable architecture of the individual LH-I and LH-II complexes, which in the case of LH-II of *Rs. molischianum* is composed of sixteen independent peptides (eight identical α-apoproteins and eight identical β-apoproteins), 24 chlorophylls, and eight carotenoids. These components self-aggregate in the cytoplasmic membrane, most likely first into heterodimers as defined above, and then, using the heterodimers as building blocks, into a ring of eight heterodimers. In the case of LH-II of *Rps. acidophila* (Duysens 1952) and *Rb. sphaeroides*, nine heterodimers aggregate into LH-II. The LH-I complex consists of sixteen heterodimers, each of which contain two chlorophylls and one carotenoid. The self-aggregation of the individual light-harvesting complexes LH-I and LH-II and of the whole PSU from its main building blocks, the heterodimers, poses a great challenge. Several questions regarding the

self-aggregation process arise: How do geometry and energetics contribute to the aggregation of two heterodimers? How is this aggregation guided in the cell membrane? How do the single heterodimer building blocks control the overall ring size? How do changes of ring size affect the stability of an overall complex? These questions might be pursued through modeling calculations; however, due to the large size of the overall ring systems and the qualitative nature of the phenomenon of self-aggregation, i.e., one does not know *a priori* what observables to monitor, I chose an approach through mechanical models of the RC, LH-I composed of sixteen heterodimers, and LH-II composed of 7–9 heterodimers. These models have been described in Bailey et al. (1998) and were used to assemble LH-II from eight heterodimer units, a most revealing experience: it turned out that the aggregation of the building blocks did not require any flexibility of the dimer surfaces; the individual components naturally fit together tightly without the need of a flexible adjustment of their surfaces. This feature implies a favorable entropy of aggregation, i.e., the heterodimers do not need to explore much conformation space to interlock. Viewing the resulting complex strikes the observer with the realization that the heterodimers have evolved purposefully corrugated self-complementary surfaces to steer the aggregation process and to stabilize the eventual aggregates. One notices that any coarse-graining of atomic level surface features of the heterodimers would deteriorate adhesion properties. In fact, the manufacturing of the models required about 30,000 triangles for the proper representation of surface features of each heterodimer; this corresponds to 1 Å resolution and proved necessary to represent properly the relevant complementarity of surfaces. The heterodimers are composed of two, rather short, transmembrane helices, a feature which requires the heterodimers to be oriented strictly normal to the membrane plane; a tilt would immerse polar side groups into the hydrophobic phase of the lipid bilayer. A pronounced top-bottom asymmetry of the heterodimer favors a vectorial orientation in the membrane. Manipulation of two heterodimer models properly juxtaposed and rotated relative to each other reveals readily the proper interlocking geometry of a pair. A similar one-dimensional (rotation around the membrane normal) search process may also govern the rapid self-assembly of LH-II in the cytoplasmic membrane. One can readily build rings of slightly "wrong" sizes, e.g., an LH-II ring of only seven or nine units, i.e., one too few or one too many. In both cases the mechanical models reveal a loose packing with wobbling heterodimer units. This is certainly a feature which results from the fact that the LH-II heterodimer models stem from the eight-ring structure of *Rs. molischianum*, i.e., a structure optimized for that particular ring size. However, the model demonstrates clearly that complementarity and orientation of the corrugated surfaces of the individual heterodimers are precise enough to control the overall ring size of eight units. I have built also the LH-I complex from sixteen models of the respective heterodimers as well as a model of the RC. This allowed me to build a key section of the PSU. The models revealed that one can readily clap the LH-I ring over the RC leading to a unique geometry of the complex. In this complex, LH-I forms an atrium-type space adjacent to the reaction center surface with the entrance of the functionally important quinone binding site. One also notices that the sixteen-unit

LH-I ring is considerably more flexible in its shape than is the eight-unit LH-II ring; it does not appear likely that the LH-I ring would assume its proper size and shape without the RC template.

SUMMARY

From a few common components, photosynthetic organisms have developed a rather divergent set of antenna systems. The evolutionary divergence has been discussed comparing the antenna systems of purple bacteria, green bacteria, cyanobacteria, dinoflagellates, and green plants in Hu et al. (1998), which contains other references on the subject. The properties of the antenna systems of purple bacteria are likely relevant for an understanding of the mechanisms common to all the mentioned light-harvesting systems. These properties are summarized here in general terms to serve potentially an understanding of a broader class of photosynthetic life forms.

The chromophores of purple bacteria, i.e., BChls and carotenoids, are attuned to their ambient light. In the case of lycopene/spheroidene and B800/B850 BChls, the combined absorption spectrum is complementary to that of chlorophyll a or b in green plants, i.e., adjusted to a habitat below plants. The purple bacteria exploit the optically allowed as well as the optically forbidden low-lying excited states of polyenes (Hudson et al. 1982; Tavan and Schulten 1987) to couple the carotenoid excitations to BChls. The carotenoids are entrusted with the excitation energy for only a few hundred femtoseconds, after which time BChls are the wardens of the energy.

The spectra of BChls are tuned only to a limited degree though interaction with the protein environment, e.g., through formylmethionine–Mg ligation in case of B800 of LH-II from *Rps. acidophila* (McDermott et al. 1995) or through an Asp–Mg ligation in case of B800 of LH-II from *Rs. molischianum* (Koepke et al. 1996); the observed spectra result mainly from intrinsic properties of BChls and excitonic interactions (Hu et al. 1997; Zerner et al. 1998). Excitonic coupling splits the excited state energies, thus improving the overlap between donor and acceptor spectra in the excitation cascade (Hu et al. 1997; Zerner et al. 1998; Damjanovic et al. 1998).

BChls have the disadvantage that their lowest energy triplet state lies high enough to excite molecular oxygen. Their companion carotenoids quench the triplet excitations of BChls.

The efficient flow of excitation through the chromophore system requires highly ordered aggregates, the geometry of which is adapted to the needed interactions; carotenoids must be in close (van der Waals) contact with BChls for triplet quenching and must be proximate within a few angstroms for transfer of optically forbidden excitations. In order to achieve significant exciton splitting, chlorophylls must have Mg–Mg distances of about 10 Å; for energy transfer on a picosecond time scale, Mg–Mg distances must be of the order of 20 Å. It is possible that BChls form aggregates to achieve coherence over many chromophores, such that the lowest energy state becomes optically forbidden, increasing its lifetime.

A multi-protein architecture is necessary to provide a large enough scaffold for the number of chromophores employed in light harvesting. Due to this architecture, antenna systems employ a hierarchy of chromophore aggregates; the chromophores are closer and more tightly coupled in the individual pigment–protein complex, e.g., in LH-II, and more loosely coupled between different pigment–protein complexes. The control of the overall aggregation of the multi-protein system is in itself an impressive achievement worthy of study.

To direct flow of excitation to the RC, the antenna system of purple bacteria assumes a spatial organization in which the BChls with lower-energy excitations are closer to the RC. Such arrangement, as shown in Figure 14.2, yields an energy funnel that prevents detours in the excitation flow, enhancing the overall efficiency of light harvesting as measured by the quantum yield for a photon absorbed to reach an RC.

The multi-protein photosynthetic apparatus as shown in Figure 14.1 poses the challenge for eventually modeling the conversion of light into ATP in its entirety. Few would have predicted that the protein constituents of the photosynthetic apparatus would be structurally known in principle already today; however, many expect that biologists will more frequently see entire protein systems engaged in complex overall functions resolved at atomic resolution. The questions posed by the photosynthetic apparatus will then be typical for biology in the 21st century: How are multiprotein systems genetically controlled? How do they physically aggregate? How did they evolve and how do they compare among species? The PSU constitutes an ideal subsystem of the photosynthetic apparatus which, due to its smaller size, is more amenable to study while posing the same principal challenges: How do LH-I and LH-II form from their many independent components? What determines the ring size and stability? How do the completed LH-IIs aggregate around the LH-I–RC complex? The function of the PSU emerges as a true system property, all components being designed to cooperate in absorbing light effectively and channel its energy to the RC. The common origin of photosynthetic, respiratory, and other organisms makes the PSU and the photosynthetic apparatus a valuable model for understanding, at the level of multiprotein systems, not only photosynthesis, but life in general.

ACKNOWLEDGMENTS

REFERENCES

Aagaard, J., and W.R. Sistrom. 1972. Control of synthesis of reaction center bacteriochlorophyll in photosynthetic bacteria. *Photochem. Photobiol.* **15**:209–225.

Alden, R.G., E. Johnson, V. Nagarajan, W.W. Parson, C.J. Law, and R.J.Cogdell. 1997. Calculations of spectroscopic properties of the LH2 bacteriochlorophyll-protein antenna complex from *Rhodopseudomonas acidophila. J. Phys. Chem. B* **101**:4667–4680.

Bailey, M., K. Schulten, and J.E. Johnson. 1998. The use of solid physical models for the study of macromolecular assembly. *Curr. Opin. Struct. Biol.* **8**:202–208.

Barvík, I., C. Warns, and P. Reineker. 1998. Exciton transfer in disordered molecular aggregates: Computer modeling of optical line shapes in ring bacteria antenna systems. *J. Luminesc.* **76/77**:331–334.

Bittl, R., and K. Schulten. 1988. Length dependence of the magnetic field modulated triplet yield of photogenerated biradicals. *Chem. Phys. Lett.* **146**:58–62.

Bittl, R., and K. Schulten. 1989. A static ensemble approximation for stochastically modulated quantum systems. *J. Chem. Phys.* **90**:1794–1803.

Chadwick, B.W., C. Zhang, R.J. Cogdell, and H.A. Frank. 1987. The effect of lithium dodecyl sulfate and sodium borohydride on the absorption spectrum of the B800–850 light-harvesting complex from *Rhodopseudomonas acidophila 7750. Biochim. Biophys. Acta* **893**:444.

Cogdell, R.J., P.K. Fyfe, S.J. Barrett, S.M. Prince, A.A. Freer, N.W. Isaacs, P. McGlynn, and C.N. Hunter. 1996. The purple bacterial photosynthetic unit. *Photosynth. Res.* **48**:55–63.

Damjanovic, A., T. Ritz, and K. Schulten. 1999. Energy transfer between carotenoids and bacteriochlorophylls in a light-harvesting protein. *Phys. Rev. E* **59**:3293–3311.

Dexter, D.L. 1953. A theory of sensitized luminescence in solids. *J. Chem. Phys.* **21**:836–850.

Dracheva, T.V., V.I. Novoderezhkin, and A. Razjivin. 1996. Exciton delocalization in the antenna of purple bacteria — Exciton spectrum calculations using x-ray data and experimental site inhomogeneity. *FEBS Lett.* **387**:81–84.

Duysens, L.N.M. 1952. Transfer of Excitation Energy in Photosynthesis. Ph.D. thesis, Utrecht.

Emerson, R., and W. Arnold. 1932. The photochemical reaction in photosynthesis. *Gen. Physiol.* **16**:191–205.

Ermler, U., G. Fritzsch, S.K. Buchanan, and U. Michel. 1994. Structure of the photosynthetic reaction center from *Rhodobacter sphaeroides* at 2.65 Å resolution: Cofactors and protein–cofactor interactions. *Structure* **2**:925–936.

Farchaus, J.W., and D. Oesterhelt. 1989. A Rhodobacter sphaeroides *puf* L, M, and X deletion mutant and its complementation in trans with a 5.3 kb *puf* operon shuttle fragment. *EMBO J.* **8**:47–54.

Fleming, G.R., and R. van Grondelle. 1997. Femtosecond spectroscopy of photosynthetic light-harvesting systems. *Curr. Opin. Struct. Biol.* **7**:738–748.

Förster, T. 1948. Zwischenmolekulare Energiewanderung und Fluoreszenz. *Ann. Phys.* (*Leipzig*) **2**:55–75.

Germeroth, L., F. Lottspeich, B. Robert, and H. Michel. 1993. Unexpected similarities of the B800–850 light-harvesting complex from Rhodospirillum molischianum to the B870 light-harvesting complexes from other purple photosynthetic bacteria. *Biochemistry* **32**:5615–5621.

Gouterman, M. 1961. Spectra of porphyrins. *J. Mol. Spectrosc.* **6**:138–163.

Hess, S., M. Chachisvilis, K. Timpmann, M.R. Jones, G.J.S. Fowler, C.N. Hunter, and V. Sundstrom. 1995. Temporally and spectrally resolved subpicosecond energy transfer within the peripheral antenna complex (LH2) and from LH2 to the core antenna complex in photosynthetic purple bacteria. *Proc. Natl. Acad. Sci. USA* **92**:12,333–12,337.

Hu, X., A. Damjanovic, T. Ritz, and K. Schulten. 1998. Architecture and function of the light-harvesting apparatus of purple bacteria. *Proc. Natl. Acad. Sci. USA* **95**:5935–5941.

Hu, X., T. Ritz, A. Damjanovic, and K. Schulten. 1997. Pigment organization and transfer of electronic excitation in the purple bacteria. *J. Phys.Chem. B* **101**:3854–3871.

Hu, X., and K. Schulten. 1997. How nature harvests sunlight. *Phys. Today* **50**:28–34.

Hu, X., and K. Schulten. 1998. A model for the light-harvesting complex I (B875) of *Rhodobacter sphaeroides*. *Biophys. J.* **75**:683–694.

Hu, X., D. Xu, K. Hamer, K. Schulten, J. Koepke, and H. Michel. 1995a. Predicting the structure of the light-harvesting complex II of *Rhodospirillum molischianum*. *Protein Sci.* **4**:1670–1682.

Hu, X., D. Xu, K. Hamer, K. Schulten, J. Koepke, and H. Michel. 1995b. Prediction of the structure of an integral membrane protein — The light-harvesting complex II of *Rhodospirillum molischianum*. In: Biological Membranes: A Molecular Perspective from Computation and Experiment, ed. K.M. Merz and B. Roux, pp. 503–533. Cambridge, MA: Birkhäuser.

Hudson, B.S., B.E. Kohler, and K. Schulten. 1982. Linear polyene electronic structure and potential surfaces. In: Excited States, ed. E.C. Lim, Vol. 6, pp. 1–95. New York: Academic Press.

Humphrey, W.F., A. Dalke, and K. Schulten. 1996. VMD — Visual Molecular Dynamics. J. Mol. Graphics **14**:33–38.

Jimenez, R., S.N. Dikshit, S.E. Bradforth, and G.R. Fleming. 1996. Electronic excitation transfer in the LH2 complex of *Rhodobacter sphaeroides*.*J. Phys. Chem*. **100**:6825–6834.

Jungas, C., J.L. Ranck, J.L. Rigaud, and A. Vermeglio. 1999. Supramolecular organization of the photosynthetic apparatus of *Rhodobacter sphaeroides*. *EMBO J.* **18**:534–542.

Karrasch, S., P.A. Bullough, and R. Ghosh. 1995. 8.5 Å projection map of the light-harvesting complex I from *Rhodospirillum rubrum* reveals a ring composed of 16 subunits. *EMBO J.* **14**:631.

Knox, K. 1963. Theory of Excitons. New York: Academic Press.

Koepke, J., X. Hu, C. Münke, K. Schulten, and H. Michel. 1996. The crystal structure of the light-harvesting complex II (B800–850) from *Rhodospirillum molischianum. Structure* **4**:581–597.

Kuhlbrandt, W. 1994. High-resolution electron crystallography of membrane proteins. In: Membrane Protein Structure: Experimental Approaches, ed. S.H. White, pp. 206–223. New York: Oxford Univ. Press.

Laible, P.D., V.C. Chynwat, M.C. Thurnauer, M. Schiffer, D.K. Hanson, and H.A. Frank. 1998. Protein modifications affecting triplet energy transfer in bacterial photosynthetic reaction centers. *Biophys. J*. **74**.2623–2637.

McDermott, G., S.M. Prince, A.A. Freer, A.M. Hawthornthwaite-Lawless, M.Z. Papiz, R.J. Cogdell, and N.W. Isaacs. 1995. Crystal structure of an integral membrane light-harvesting complex from photosynthetic bacteria. *Nature* **374**:517–521.

Miller, K.R. 1982. Three-dimensional structure of a photosynthetic membrane. *Nature* **300**:53–55.

Monger, T.G., and W.W. Parson. 1977. Singlet-triplet fusion in *Rhodopseudomonas sphaeroides* chromatophores. A probe of the organization of the photosynthetic apparatus. *Biochim. Biophys. Acta* **460**:393–407.

Nagae, H., T. Kakitani, T. Katoh, and M. Mimuro. 1993. Calculation of the excitation transfer matrix elements between the S_2 or S_1 state of carotenoid and the S_2 or S_1 state of bacteriochlorophyll. *J. Chem. Phys.* **98**:8012–8023.

Oppenheimer, J.R. 1941. Internal conversion in photosynthesis. *Phys. Rev.* **60**:158.

Pullerits, T., and V. Sundstrom. 1996. Photosynthetic light-harvesting pigment–protein complexes: Toward understanding how and why. *Acc. Chem. Res.* **29**:381–389.

Ricci, M., S.E. Bradforth, R. Jimenez, and G.R. Fleming. 1996. Internal conversion and energy transfer dynamics of spheroidene in solution and in the LH-1 and LH-2 light-harvesting complexes. *Chem. Phys. Lett.* **259**:381–390.

Ritz, T., X. Hu, A. Damjanovic, and K. Schulten. 1998. Excitons and excitation transfer in the photosynthetic unit of purple bacteria. *J. Luminesc.* **76/77**:310–321.

Sauer, K., R.J. Cogdell, S.M. Prince, A. Freer, N.W. Isaacs, and H. Scheer. 1996. Structure-based calculations of the optical spectra of the LH2 bacteriochlorophyll-protein complex from *Rhodopseudomonas acidophila. Photochem. Photobiol.* **64**:564–576.

Schulten, K., and M. Tesch. 1991. Coupling of protein motion to electron transfer: Molecular dynamics and stochastic quantum mechanics study of photosynthetic reaction centers. *Chem. Phys.* **158**.421–446.

Shreve, A.P., J.K. Trautman, H.A. Frank, T.G. Owens, and A.C. Albrecht. 1991. Femtosecond energy-transfer processes in the B800–850 light-harvesting complex of *Rhodobacter sphaeroides* 2.4.1. *Biochim. Biophys. Acta* **1058**:280–288.

Tavan, P., and K. Schulten. 1987. Electronic excitations in finite and infinite polyenes. *Phys. Rev. B* **36(8)**:4337–4358.

Thompson, M., and M. Zerner. 1991. A theoretical examination of the electronic structure and spectroscopy of the photosynthetic reaction center from *Rhodopseudomonas viridus*. *J. Am. Chem. Soc.* **113**:8210–8215.

van Grondelle, R., J. Dekker, T. Gillbro, and V. Sundstrom. 1994. Energy transfer and trapping in photosynthesis. *Biochim. Biophys. Acta* **1187**:1–65.

van Oijen, A.M., M. Ketelaars, J. Kohler, T.J. Aartsma, and J. Schmidt. 1999. Unraveling the electronic structure of individual photosynthetic pigment-protein complexes. *Science* **285**:400–402.

Visscher, K.J., H. Bergstrom, V. Sundstrom, C.N. Hunter, and R. van Grondelle. 1989. Temperature dependence of energy transfer from the long wavelength antenna BChl-896 to the reaction center in *Rhodospirillum rubrum*, *Rhodobacter sphaeroides* (w.t and m21 mutant) from 77 to 177 k, studied by picosecond absorption spectroscopy. *Photosynth. Res.* **22**:211–217.

Walz, T., and R. Ghosh. 1997. Two-dimensional crystallization of the light-harvesting I-reaction centre photounit from *Rhodospirillum rubrum. J. Mol. Biol.* **265**:107–111.

Wu, H.-M., N.R.S. Reddy, and G.J. Small. 1997. Direct observation and hole burning of the lowest exciton level (B870) of the LH2 antenna complex of *Rhodopseudomonas acidophila* (strain 10050). *J. Phys. Chem. B* **101**:651–656.

Xu, D., and K. Schulten. 1994. Coupling of protein motion to electron transfer in a photosynthetic reaction center: Investigating the low temperature behaviour in the framework of the spin-boson model. *Chem. Phys.* **182**:91–117.

Zerner, M.C., M.G. Cory, X. Hu, and K. Schulten. 1998. Electronic excitations in aggregates of bacteriochlorophylls. *J. Phys. Chem.* B **102**:7640–7650.

Zuber, H., and R.A. Brunisholz. 1991. Structure and function of antenna polypeptides and chlorophyll-protein complexes: Principles and variability. In: Chlorophylls, ed. H. Scheer, pp. 627–692. Boca Raton: CRC Press.

Standing, left to right: Helmut Grubmüller, Ugo Palma, Arieh Warshel, Uli Nienhaus
Seated, left to right: Don Crothers, Keith Moffat, Klaus Schulten, Fritz Parak
Not pictured: Jean-Pierre Changeux